Bulgarian Journal of Physics vol. **48** (2021) 505–513

Cluster Radioactivity Study of Transition Metal Region Using RMF theory

Ajeet Singh, **A. Shukla**

Department of Physics, Rajiv Gandhi Institute of Petroleum Technology, Jais, Amethi – 229304, India

Received *15 October 2021*

Abstract. We have studied the clusters (^{12}C, ^{16}O, and ^{20}Ne) decay half-lives in the transition metal region ($^{158–170}$W, $^{160–174}$Os, and $^{166-178}$Pt, respectively). These half-lives have been calculated using the effective liquid drop model (ELDM) of cluster decay in conjunction with the relativistic mean-field (RMF) model with the NL3* parameter set. Thus calculated cluster decay half-lives are also compared with the half-lives computed using the latest empirical relations, namely Universal decay law (UDL) and the Scaling Law was given by Horoi *et al*. From the calculated results, it has been observed that in the transition metal region, half-lives are minimum at $N_d = 82$ (N_d is the neutron number of the daughter nuclei), which is a magic number and shell effect at $N_d = 82$. Further, the Geiger-Nuttal plots of half-lives showing Q-value dependence for different alpha-like clusters from various CR emitters that have been plotted are found to vary linearly.

KEY WORDS: cluster decay; effective liquid drop model; Geiger-Nuttall plots; Q-value; relativistic mean-field; transition metal.

1 Introduction

Cluster radioactivity was first observed theoretically in 1980 by Sandulescu, Poenaru, and Greiner [1] based on fragmentation theory. In this new type of exotic radioactive decay, i.e., the cluster radioactivity process, the parent nuclei emit a particle heavier than alpha particle and lighter than the lightest fission fragments [2]. Later in 1984, the first experimental signature of cluster radioactivity was observed via the spontaneous emission of ^{14}C cluster from the decay of ^{223}Ra by Rose and Jones [3]. Subsequently, cluster decay has been experimentally observed in different nuclei of the trans-lead region (Z=87-96), namely for the cluster decay of ^{14}C, ^{18,20}O, ^{23}F, ^{22,24,26}Ne, ^{28,30}Mg, and ^{32,34}Si [4]. In this region, all cluster emissions have a doubly magic nucleus of ^{208}Pb ($Z = 82$,

$N = 126$) or its neighboring nuclei as the daughter nuclei. In the recent past, two new islands of emission of clusters have been predicted by several theoretical models, first in the superheavy region and second in the trans-tin region ($Z = 56$–64) [5, 6]. For the parent nuclei lying in the trans-tin region ($Z = 56$-64), it has been observed that daughter nuclei lie close to doubly magic nuclei ^{100}Sn ($Z = 50$, $N = 50$) [7]. It is important to note that the first experimental observation of cluster decay from the trans-tin region has been already confirmed by Oganessian *et al.* [8] at Dubna (Russia) and by Guglielmetti *et al.* [9] at GSI (Germany) in 1995.

The cluster decay is described using two different types of approaches. The first one is known as Performed cluster model [6], and the other is a fission-based model. In Performed cluster model, it is assumed that the cluster is made of several nucleons are performed in the parent nucleus before they could tunnel through the barrier created by the nuclear and Coulomb potentials. In the fission-based model, Gamaw's idea of quantum mechanical barrier penetration is still used. The shape parametrization is chosen as fission-like, where the decaying system is considered as two intersecting spheres of different radii which are used to describe the decaying fragments.

In the present work, we have used the Effective Liquid Drop Model (ELDM) [10, 11] to determine the cluster decay half-lives, using mass excess data calculated from the relativistic mean-field model (NL3* parameter set). We have calculated the binding energy per nucleon (B.E./A) of various isotopes of even-even parent nuclei, daughter nuclei, and emitted clusters using RMF (NL3* parameter set) model. The mass excess data (ΔM) for cluster decay is evaluated by making use of these binding energy per nucleon. This mass excess data (ΔM) has been used further as input to obtain a Q-value and determine the cluster decay half-lives with the Effective Liquid Drop Model. Further, to check the prediction ability, we have compared our results with the available experimental results and other theoretical calculations including the ones that use the empirical formula Universal Decay Law (UDL) and the Scaling Law by Horoi *et al.*. Also, the Geiger-Nuttall plots of $Q^{(-1/2)}$ and $-\ln P$ versus $\log_{10} T_{1/2}$ for emission of ^{12}C, ^{16}O, and ^{20}Ne clusters for various isotopes of parent nuclei have been analyzed.

2 Mathematical Formalism

2.1 Relativistic mean field model

The RMF model is the relativistic lagrangian density functional for a nucleon-meson many-body system which is given as [12, 13]

$$\mathcal{L} = \overline{\Psi_i}[i\gamma^\mu\partial_\mu - M]\Psi_i + \frac{1}{2}\partial^\mu\sigma\partial_\mu\sigma - \frac{1}{2}m_\sigma^2\sigma^2 - \frac{1}{3}g_2\sigma^3 - \frac{1}{4}g_3\sigma^4$$
$$- g_s\overline{\Psi_i}\Psi_i\sigma - \frac{1}{4}\Omega^{\mu\nu}\Omega_{\mu\nu} + \frac{1}{2}m_\omega^2V^\mu V_\mu + \frac{1}{4}c_3(V_\mu V^\mu)^2 - g_w\overline{\Psi_i}\gamma^\mu\Psi_i V_\mu$$
$$- \frac{1}{4}\overrightarrow{B}^{\mu\nu}.\overrightarrow{B}_{\mu\nu} + \frac{1}{2}m_\rho^2\overrightarrow{R}^\mu.\overrightarrow{R}_\mu - g_\rho\overline{\Psi_i}\gamma^\mu\overrightarrow{\tau}\Psi_i.\overrightarrow{R}^\mu$$
$$- \frac{1}{4}F^{\mu\nu}F_{\mu\nu} - e\overline{\Psi_i}\gamma^\mu\frac{(1-\tau_{3i})}{2}\Psi_i A_\mu. \quad (1)$$

Here σ, V_μ and $\overrightarrow{R}_\mu$ are the fields for isoscalar-scalar σ-meson, isoscalar-vector ω-meson, and isovector-vector ρ-meson, respectively. The ψ_i are the Dirac spinors for the nucleons whose third component of isospin is denoted by τ_{3i}. Here g_σ, g_ω, g_ρ and $e^2/4\pi = 1/137$ are the coupling constants for σ, ω, ρ mesons and photons, respectively. g_2, g_3, and c_3 are the parameters for the nonlinear terms of σ and ω mesons. This model predicts good results of binding energy, root mean square radius, quadrupole deformation parameter not only for stable nuclei but also for nuclei throughout the periodic table. A version of the RMF model, especially with the NL3 effective interaction (or with a slightly improved version, i.e., NL3* effective interaction) has been used in many nuclear reactions and structure studies.

2.2 Effective liquid drop model of cluster decay

In the present work, we have used the effective liquid drop model given by M. Gonclaves *et al.* [10, 11]. We have used the Shi and Swiatecki [14] hindrance for even-even parent nuclei, and P is the penetrability factor for one-dimension barrier used in shape parameterization of the dinuclear system calculated by equation

$$P = exp\left[\frac{-2}{\hbar}\int_{\zeta_0}^{\zeta_c}\sqrt{2\mu[V(\zeta)-Q]}d\zeta\right], \quad (2)$$

where μ is the inertial coefficient and Q is the energy released in the cluster decay. Here, the Q-value of reaction is calculated by mass excess data through RMF (NL3* parameter set) calculations. The effective one-dimensional potential energy can be calculated using this relation

$$V = V_c + V_s + V_l. \quad (3)$$

Here V_c, V_s and V_l are the Coulomb, surface and Centrifugal potentials.

The half-life for the cluster decay is given as

$$T_{1/2} = \left(\frac{ln2}{\lambda}\right), \quad (4)$$

where λ is the radioactive decay rate given by

$$\lambda = \nu P. \quad (5)$$

In Eq. (5) $\nu = (\frac{2E_\nu}{h})$ is the parameter for assault frequency of the barrier. More details of shape parametrization, e.g., the effective surface tension of liquid drop and the inertia tensor, can be found in the literature [10, 11, 15].

2.3 Half-lives using empirical formula

2.3.1 The Universal Decay Law (UDL)

The UDL formula holds for the monopole radioactive decays of all clusters. The model is dependent on the mass, charge numbers of the daughter and emitted clusters, and the Q-value. The UDL formula [6, 16] is given by the expression

$$\log_{10} T_{1/2}(\text{UDL}) = aZ_eZ_d\sqrt{\frac{\mu}{Q}} + b\sqrt{\mu Z_eZ_d(A_e^{1/3} + A_d^{1/3})} + c\,, \quad (6)$$

where $\mu = A_eA_d/(A_e + A_d)$ is the reduced mass and A_e, A_d are the mass numbers of daughter and emitted cluster, respectively. The three coefficient sets of Eq. (6) are $a = 0.3949$, $b = -0.3693$, and $c = -23.7615$.

2.3.2 Scaling law of Horoi *et al.*

We have calculated the half-life of cluster decays using the empirical formula given by M. Horoi *et al.* [17, 18] in terms of reduced mass μ, and the constants a, b, c, and d are the coefficients set (see, for details, Refs. [6, 17, 18]):

$$\log_{10} T_{1/2}(\text{Horoi}) = (a\mu^{0.416}+b)[(Z_eZ_d)^{(0.613)}/\sqrt{Q}-7]+(c\mu^{0.416}+d)\,, \quad (7)$$

where $T_{1/2}$ is the cluster decay half-life and Z_d and Z_e represent the atomic number of the daughter and emitted nucleus. The four coefficient sets are $a = 9.1$, $b = -10.2$, $c = 7.39$, and $d = -23.2$.

3 Results and Discussion

We have studied the cluster decay half-lives in the emission of alpha-like (^{12}C, ^{16}O, and ^{20}Ne) clusters from various even-even parent nuclei ($^{158–170}$W, $^{160–174}$Os, and $^{166–178}$Pt, respectively). The mass defect and Q-values needed for cluster decay half-lives determination are calculated using the RMF model with NL3* parameter [12, 13]. Further, the calculation of cluster decay half-lives have been done using the Effective Liquid Drop Model (ELDM) [10, 11]. We used a combination of the Varying mass Asymmetry Shape and Werner-Wheeler's inertia in the Effective Liquid Drop Model. It is to be noted here that all cluster decay half-lives calculations in ELDM have been performed here by using zero angular momenta.

We have determined the mass excess data (ΔM) by using the binding energy per nucleon in RMF (NL3* parameter set). The relation between binding energy per nucleon and mass excess data is given by

Mass of the Nuclei = ((N*M_n +Z*M_p)*931.5 - A*B.E./A)/931.5

ΔM = (Mass of the Nuclei - Mass No. of Nuclei)*931.5 .

To calculate the Q-value, we used mass excess data of RMF (NL3*) and FRDM. The following relation is given by:

$$Q(N,Z) = \Delta M_p(N,Z) - [\Delta M_d(N,Z) + \Delta M_e(N,Z)]\,. \tag{8}$$

Here $\Delta M_p(N,Z)$ is the mass excess of the parent nucleus, $\Delta M_d(N,Z)$, $\Delta M_e(N,Z)$ are the mass excess of the daughter and cluster, respectively. The finite-range-droplet model (FRDM) mass excess data are taken from Ref. [19]. The positive Q-value ($Q > 0$) for all possible combinations (parent and cluster) have been considered. In the present study, we have compared the prediction ability of various models used for cluster decay half-lives. For this, we have compared the results obtained by the ELDM model with the results obtained by empirical formula, namely the UDL and Scaling Law by Horoi *et al.*. Further, to compare the impact of the various Q-values, we have also compared calculated half-lives using ELDM by two sets of Q-values obtained from RMF calculations, as well as from FRDM data.

It can be seen from Figure 1, that for the cluster decay of ^{12}C from $^{158-170}$W isotopes, the Q-value has a maximum for daughter nuclei ^{150}Er ($Z_d = 68, N_d = 82$). For the cluster decay of ^{16}O from $^{160-174}$Os, the Q value has a maximum for daughter nuclei ^{150}Er ($Z_d = 68, N_d = 82$) and similarly ^{20}Ne decay from $^{166-178}$Pt, the Q-value has a maximum for daughter nuclei ^{150}Er ($Z_d = 68, N_d = 82$). The analyses of Figure 1, clearly show that the calculated Q-value indicates shell effects due to magic number of nucleons (N_d = 82)

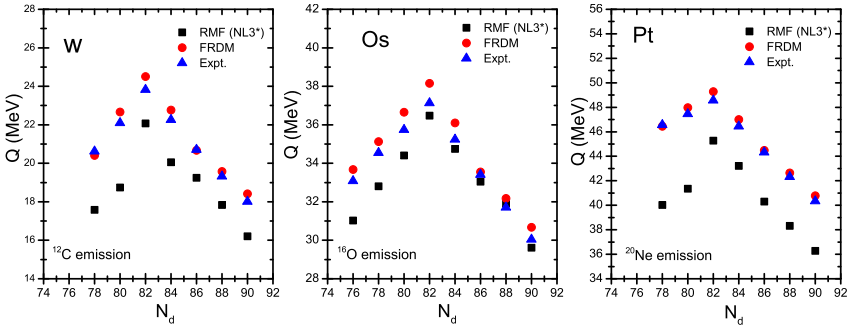

Figure 1. (Color online) The Q-value for the clusters (^{12}C, ^{16}O, and ^{20}Ne) decay from $^{158–170}$W, $^{160–174}$Os, and $^{166–178}$Pt isotopes using RMF (NL3* parameter set) model compared with the FRDM [19] and experimental data [20], wherever available.

and affects the half-lives. As the size of the α-like cluster increases, the Q-value also increases. The calculated Q-values from RMF (NL3* parameter set) are compared with FRDM values. The calculated Q-values using RMF (NL3*) are slightly lower than the FRDM values and experimental data because of a small change in the values of a parameter of NL3* and FRDM will affact the values of binding energy per nucleon.

The half-lives of the alpha-like clusters (^{12}C, ^{16}O, and ^{20}Ne) decay from $^{158–170}$W, $^{160–174}$Os, and $^{166–178}$Pt isotopes (transition metal region) within the ELDM (NL3*), UDL, and scaling Law by Horoi *et al.* and are compared with the ELDM (FRDM) as well as UNIV values [21]. The decay half-lives calculated using RMF (NL3*), UDL, and the scaling law of Horoi and their comparisons are given in Figure 2(a, b, and c). Figure 2(a) shows the plot for the cluster decay half-lives versus the neutron number of the daughter in the emission of ^{12}C from $^{158-170}$W isotopes. Here the cluster decay half-lives are found to have minima for the decay leading to daughter nuclei ^{150}Er ($Z_d = 68, N_d = 82$), which has magic neutron number $N_d = 82$. Figure 2(b) presents the cluster decay of ^{16}O from $^{160-174}$Os isotopes. The cluster decay half-lives are found to have a minimum value for the decay leading to magic daughter nuclei ^{150}Er ($Z_d = 68, N_d = 82$). Similarly, Figure 2(c) shows the cluster decay of ^{20}Ne from $^{166-178}$Pt isotopes. The minima of the cluster decay half-lives are found for the decay leading to magic daughter nuclei ^{150}Er ($Z_d = 68, N_d = 82$). The minimum value in the cluster decay half-lives corresponds to the higher barrier penetrability, which shows the doubly magic character (proton/neutron shell closure) of the daughter nuclei. In the present studies on transition metal region, it has been found that the decay half-lives has a minimum value for the decay leading to the magic daughter nuclei $N_d = 82$. These observations re-

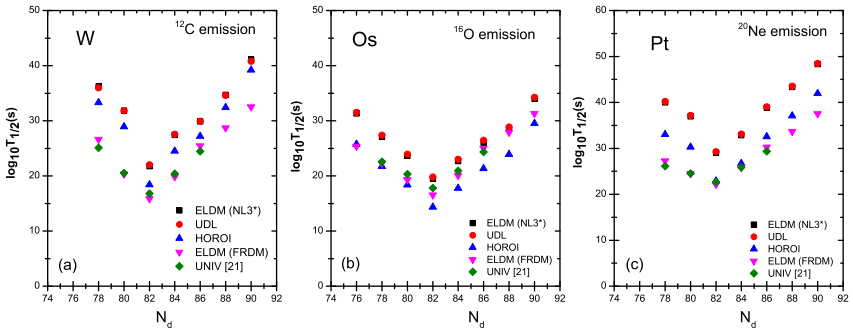

Figure 2. (Color online) Plot of the computed $\log_{10} T_{1/2}$ versus neutron number of a daughter, N_d, for the emission of clusters ^{12}C, ^{16}O, and ^{20}Ne from W, Os, and Pt isotopes, respectively. The logarithm of half-lives have been calculated using the ELDM (by inputting NL3* and FRDM values) and empirical formulas UDL, Horoi (using NL3* Q-values). The UNIV data are taken from Ref [21].

veal the role of the strong shell effects in cluster radioactivity. We can see from Figure 2(a, b, and c) that the half-lives ($\log_{10} T_{1/2}$) versus neutron number of daughter nuclei N_d reveal the fact that the ELDM (NL3*), UDL, Scaling Law by Horoi *et al.*, ELDM (FRDM) and UNIV values [21] exhibit almost similar trends in all plots. The obtained results using ELDM (NL3*) are compared with the empirical formula UDL and Scaling low of Horoi *et al.*. It is found that ELDM (NL3*) and UDL values are almost the same but a small discrepancy is observed in the results obtained by the Scaling Law of Horoi. Because the Horoi formula is the simple scaling law and the coefficient sets are estimated by fitting the experimental data with the parent charge number $Z = 87$–96 only. Although small nuclear structure information is taken into account, their prediction power is not good. But UDL formula is derived from the α-like R-matrix theory, so its prediction accuracy is close to the microscopic results.

In 1911 Geiger and Nuttall experimentally confirmed the relation between the decay constant λ and the disintegration energy Q of various decay modes, which is the Geiger-Nuttall law [22, 23]. Figure 3(a) shows the Geiger-Nuttall plots for half-lives ($\log_{10} T_{1/2}$) versus $Q^{-1/2}$ (Q in MeV) for the different clusters (^{12}C, ^{16}O, and ^{20}Ne) emitted from the parents $^{158–170}$W, $^{160–174}$Os, and $^{166–178}$Pt isotopes. A linear behavior in each case is clearly shown in Figure 3(a). The Geiger-Nuttall law is written in the form

$$\log_{10} T_{1/2} = \frac{X}{\sqrt{Q}} + Y \,, \tag{9}$$

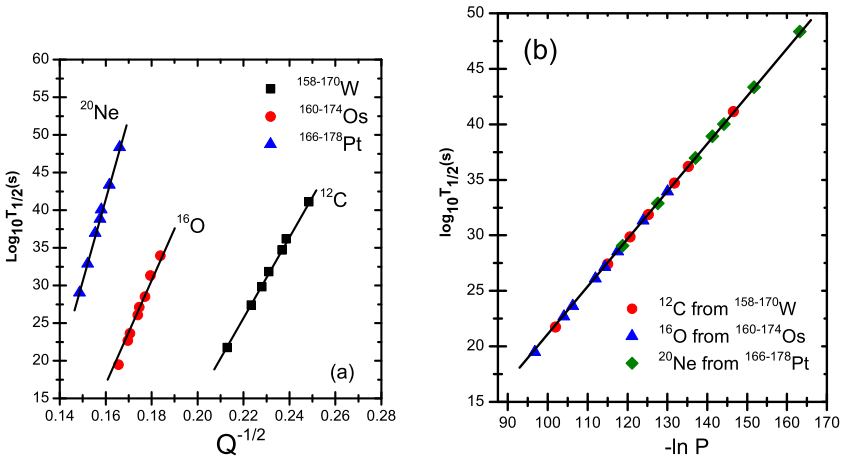

Figure 3. (Color online) (a) Geiger-Nuttall plot of half-lives vs. $Q^{-1/2}$ for various clusters from W, Os, and Pt isotopes. (b) Universal curve for calculated $\log_{10} T_{1/2}$ (in s) vs. negative logarithm of penetrability (-ln P) for alpha-like clusters (^{12}C, ^{16}O, and ^{20}Ne) decay from different parent nuclei.

where X and Y are the slopes and intercepts of the straight lines, respectively. We would like to point out that the G-N law is appropriate in the case of the mode under pure Coulomb potential. The calculated results plots reveal that the inclusion of surface potential and shell effect (through Q-value) will not produce a significant variation to the straight-line behavior. Each emitted alpha-like cluster has a distinct slope and intercept.

We have shown the plot (Universal curve) between logarithmic half-lives against the negative logarithm of penetrability (-$\ln P$). The universal curves for ^{12}C from $^{158-170}$W, ^{16}O from $^{160–174}$Os and ^{20}Ne from $^{166–178}$Pt have been given in Figure 3(b). Here, the graph is found to be linear behavior with nearly equal slope (slop = 0.457) and intercept (intercept = - 20.923), which exhibit that the assault frequency is almost a constant for all clusters decay.

4 Conclusion

In summary, we have studied the Q-values and cluster decay half-lives for even-even CR nuclei in the transition metal region ($^{158–170}$W, $^{160–174}$Os, and $^{166–178}$Pt) using relativistic mean-field (RMF) model with NL3* parameter set and empirical formulas: UDL and Scaling Law by Horoi *et al.*. The Effective Liquid Drop Model of cluster decay has been used to calculate cluster decay half-lives.

The calculated Q-value has a maximum for near magic daughter nuclei ^{150}Er ($Z = 68$, $N = 82$) in the transition metal region, the Q-value has a maximum for neutron number of daughter nuclei $N_d = 82$, which is a magic number. The calculated Q-value indicates the shell effects at $N_d = 82$ and influences the half-lives. In the transition metal region, the minima of the cluster decay half-lives are found for the decay leading to magic daughter nuclei ^{150}Er ($Z = 68$, $N = 82$). The calculated half-lives of cluster decay using ELDM (NL3*) are compared with the values of empirical formula UDL and Scaling Law by Horoi *et al.*. It is found that our results obtained with ELDM in conjunction with RMF are close to the results obtained with the UDL formula. It can be seen that the prediction power of the scaling law of Horoi is limited. But UDL formula is derived from the α-like R-matrix theory, so their prediction accuracy is closed to the once by the NL3* results. Also, calculated results are in good agreement with the experimental data. The decay constant λ for a cluster decay will be maximum if the corresponding logarithmic half-life is minimum. The Geiger-Nuttal plots clearly show a linear behavior with different slopes and intercepts for various α-like clusters decay from various parents nuclei. We concluded that the RMF (NL3*) formalism provides appropriate good results for all the considered isotopes. The present study of cluster decays of these isotopes may be helpful for future experiments.

Acknowledgement

Ajeet Singh is highly thankful to the Council of Scientific and Industrial Research, New Delhi for providing Senior Research Fellowship (SRF) under file no.: 09/1088(0005)/2018-EMR-I.

References

[1] A. Sandulescu, D.N. Poenaru, W. Greiner (1980) *Sov. J. Part. Nucl.* **11** 528.
[2] S.K. Arun, R.K. Gupta, B.B. Singh, S. Kanwar, M.K. Sharma (2009) *Phys. Rev. C* **79** 064616.
[3] H.J. Rose, G.A. Jones (1984) *Nature (London)* **307** 245.
[4] P.B. Price (1989) *Annu. Rev. Nucl. Part. Sci.* **39** 19.
[5] K.P. Santhosh, I. Sukumaran (2017) *Eur. Phys. J. A* **53** 136.
[6] Y. Gao, J. Cui, W. Yanzhao, J. Gu (2020) *Sci. Rep.* **10** 9119.
[7] K. Manimaran and M. Balasubramaniam (2009) *Int. J. Mod. Phys. E* **18** 1509-1520.
[8] Yu. Tu Oganessian, Yu.A. Lazarev, V.L. Mikheev, Yu.A. Muzychka, L.V. Shirokovsky, S.P. Tretyakova, V.K. Utyonkov (1994) *Z. Phys. A* **349** 341.
[9] A. Guglielmetti, *et al.* (1995)*Phys. Rev. C* **52** 740.
[10] M. Goncalves, S.B. Duarte (1993) *Phys. Rev. C* **48** 2409.
[11] M. Goncalves, S.B. Duarte, F. Garcia, O Rodriguez (1997) *Comput. Phys. Commin.* **107** 246-252.
[12] S.K. Patra, C.R. Praharaj (1991) *Phys. Rev. C* **44** 2552.
[13] A. Shukla, Sven Aberg, S.K. Patra (2011) *J. Phys. G: Nucl. Part. Phys.* **38** 095103.
[14] Y.J. Shi, W.J. Swiatecki (1987) *Nucl. Phys. A* **464** 205.
[15] J.P. Cui, Y.L. Zhang, S. Zhang, Y.Z. Wang (2018) *Phys. Rev. C* **97** 014316.
[16] C. Qi, *et al.* (2009) *Phys. Rev. C* **80** 044326.
[17] M. Horoi, A. Brown, A. Sandulescu (1994) arXiv: nucl-th/9403008v1.
[18] M. Horoi (2004) *J. Phys. G: Nucl. Part. Phys.* **30** 945.
[19] P. Moller, A.J. Sierk, T. Ichikawa, H. Sagawa (2016) *At. Data and Nucl. Data Tables* **109** 1.
[20] National Nuclear Data Center (NNDC) in Brookhaven National Laboratory, http://www.nndc.bnl.gov.
[21] K.E. Abd El Mageed, *et al*. (2015) *Chin. J. Phys.* **53** 120304.
[22] H. Geiger, J.M. Nuttall (1911) *Philos. Mag.* **22** 613.
[23] H. Geiger (1922) *Z. Phys.* **8** 45.